

nffa.eu

**PILOT** 2021  
2026

## **DELIVERABLE REPORT**

---

WPN WP Title

**D12.3**

# **First demonstration of OAM beams at HHG source**



This initiative has received funding from the EU's H2020 framework program for research and innovation under grant agreement n. 101007417, NFFA-Europe Pilot Project

## PROJECT DETAILS

PROJECT ACRONYM

PROJECT TITLE

NEP

Nanoscience Foundries and Fine Analysis - Europe|PILOT

GRANT AGREEMENT NO:

FUNDING SCHEME

101007417

RIA - Research and Innovation action

START DATE

01/03/2021

## WORK PACKAGE DETAILS

WORK PACKAGE ID

WORK PACKAGE TITLE

12

JA2 – X-ray Wavefront Metrology, Correction and Manipulation

WORK PACKAGE LEADER

Prof. Christian David (PSI)

## DELIVERABLE DETAILS

DELIVERABLE ID

DELIVERABLE TITLE

D – D12.3

First demonstration of OAM beams at HHG source

DELIVERABLE DESCRIPTION

The deliverable is connected to the task 12.3 "Development of phase manipulation techniques for OAM X-ray beams" (involving DESY, PSI and UNG), which aims at producing and characterizing OAM beams both at HHG and FEL sources. OAM beams with different topological charge have been generated, characterized and optimized at the FERMI FEL. The developed techniques can be easily transferred to HHG sources.

DUE DATE

ACTUAL SUBMISSION DATE

M24 02/28/2023

17/03/2023

AUTHORS

Prof. Giovanni De Ninno (UNG)



## PERSON RESPONSIBLE FOR THE DELIVERABLE

---

Prof. Giovanni De Ninno (UNG)

## NATURE

---

R - Report

P - Prototype

DEC - Websites, Patent filing, Press & media actions, Videos, etc

O - Other

## DISSEMINATION LEVEL

---

P - Public

PP - Restricted to other programme participants & EC: (Specify)

RE - Restricted to a group (Specify)

CO - Confidential, only for members of the consortium



## REPORT DETAILS

ACTUAL SUBMISSION DATE

17/03/2023

NUMBER OF PAGES

9 (right-click and select "update the field")

FOR MORE INFO PLEASE CONTACT

Giovanni De Ninno,  
University of Nova Gorica  
Vipavska 11c  
SI-5270 Ajdovščina, Slovenija

email: giovanni.deninno@ung.si

VERSION	DATE	AUTHOR(S)	DESCRIPTION / REASON FOR MODIFICATION	STATUS
1	DD/MM/YYYY			Draft
				Choose an item.
				Choose an item.
				Choose an item.
				Choose an item.
				Choose an item.
				Choose an item.



# Introduction

We implemented two methods for generating intense XUV beams carrying OAM. In the first one, in situ, we took advantage of the vortex nature of harmonics emitted in a helical undulator of a free-electron laser (FEL). For that, we exploited high-harmonic and nonlinear harmonic generation to obtain intense, femtosecond, coherent XUV vortices from a chain of six undulators at the FERMI FEL. The method can be easily implemented at other existing FEL facilities. The second technique, ex situ, relies on the use of a spiral zone plate (SZP), which is placed directly into the FEL beam path. The setup produces a focused, micron-sized, high-intensity optical vortex without requiring extensive modifications of the FEL beamline. The latter method can be also used to generate OAM light, with variable topological charge, using a high-order harmonic generation (HHG) source.

In the following, we review the results obtained using both in situ and ex situ methods for generating, characterizing and optimizing FEL light carrying OAM.

## In-situ generation of UV pulses with OAM

Theoretical studies demonstrated that vortex beams emitted by free electrons are more ubiquitous than previously thought. Indeed, harmonic components of radiation produced by a relativistic electron moving on a circular or spiral trajectory, such as the one in a helical undulator, carry a total (spin and orbital) angular momentum of  $n\hbar$  per photon, where  $n$  is the harmonic number. In the paraxial regime, this translates into an OAM content corresponding to  $P=n-1$ . Although it has been known for a while that harmonics emitted by a helical undulator show a characteristic donut-like distribution with zero on-axis intensity, the helical phase of such radiation has only recently been addressed in more detail. The experiment was performed at the FERMI FEL. An ultraviolet (250-nm) seed laser was used to energy modulate the e-beam in the first undulator (modulator), as shown in Fig.1.

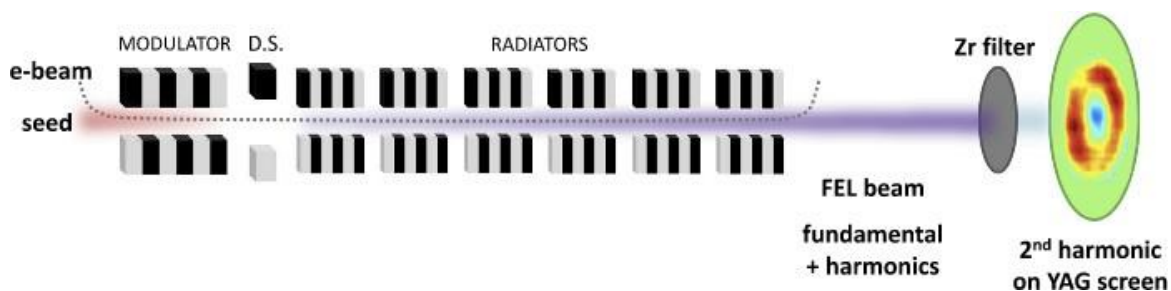


Fig. 1: Generation of coherent optical vortices through nonlinear harmonic generation at a FEL (not to scale). A transversely Gaussian seed density modulates the e-beam using a combination of an undulator (modulator) and a dispersive section (D.S.) so that it emits coherent XUV light in the radiator. The interaction between FEL radiation at the fundamental wavelength and the e-beam induces bunching at the second harmonic, which is amplified along the radiator chain, leading to emission of intense, coherent optical vortices in the XUV spectral range. A Zr filter is placed at the FEL output to suppress the fundamental Gaussian mode, transmitting only the optical vortex.

The e-beam was then sent through a dispersive section (a four-dipole-magnet chicane), where the energy modulation was transformed into a current-density modulation (bunching) with Fourier components spanning many harmonics of the seed laser frequency. Such a bunched e-beam entered the helical radiator tuned to a fundamental wavelength of 37.8 nm (i.e., the eighth harmonic of the seed), producing coherent light in the XUV. The FEL was operated in the high-gain

regime, close to the saturation point[39,40]. Under these conditions, the interaction between the radiation at the fundamental FEL wavelength and the e-beam induces bunching at the second harmonic (18.9 nm). The resulting coherent emission was amplified along the whole undulator chain, giving intensities at the second harmonic on the order of  $10^{-3}$  of the fundamental FEL intensity. The electron trajectory was carefully aligned using the fundamental emission (Gaussian mode) from each radiator. The transverse intensity distribution was collected 50 m downstream from the last radiator by inserting a YAG screen, which was imaged by a CCD camera.

To confirm the vortex nature of the emitted light, we performed an interference experiment by tuning the first undulator to a resonant wavelength corresponding to the second harmonic of the following undulators. The interference between the Gaussian mode produced by the first radiator section and the OAM-carrying light from the rest of the undulators gave a single spiral structure, a clear proof that the vortex beam carried a topological charge of  $P = n - 1 = 1$ , as shown in the Fig. 2 (left). By changing the phase between the two (Gaussian and OAM) beams, a rotation of the spiral is observed. By quantifying the amount of rotation, one can correlate the phase of the OAM with the strength of the phase shifter at the exit of the first undulator.

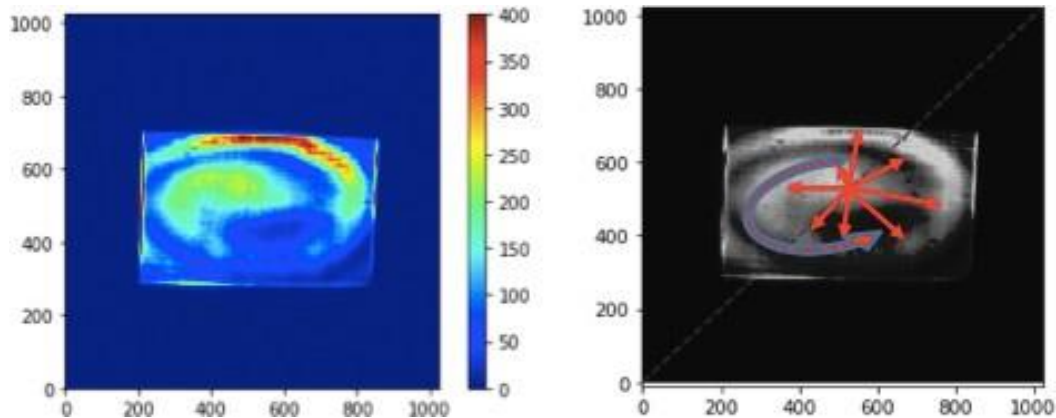


Fig. 2: A single-spiral pattern obtained by interference of the optical vortex with a Gaussian mode, confirming the  $P = 1$  charge of the vortex beam.

The evolution of the radius along the spiral structure is a characteristic quantity that can be associated with the rotation of the spiral, see Fig. 2 right. The radius was taken as the distance between the central pixel (#512) and the peaks along cut line, whose slope was varied to get a full 360-degree rotation along the spiral. In this way, the rotation of the spiral was quantified: an oscillatory trend was found, with two complete rotations ( $4\pi$ ) in the range of the values of interest, see Fig. 3.

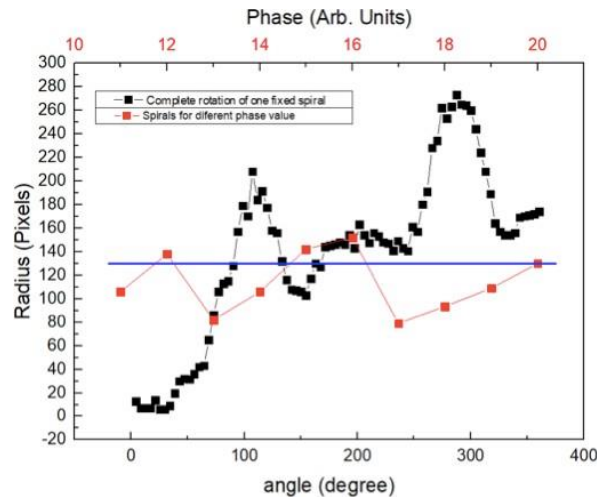


Fig. 3: Values of radii along the spiral structure. Black squares: radii obtained from the spiral shown in Fig. 2, for different slopes of the cut line (horizontal bottom scale). Red squares: radii for spirals obtained (for a fixed slope of the cut line) using different strengths of the phase shifter between the first undulator and the following ones. Different strengths of the phase shifter correspond to different phases between Gaussian and OAM emissions (horizontal top scale).

## Ex-situ generation of UV pulses with OAM

A high-intensity optical vortex can also be obtained by placing a SZP directly into the optical path of the fundamental (transversely Gaussian) FEL beam. The SZP simultaneously imprints a helical phase onto the FEL beam and focuses it, generating a focused optical vortex. OAM beams with different topological charge were generated and characterized at the DiProI beamline of the FERMIFEL source, using SZPs fabricated at PSI. The produced radiation was then used for an experiment of ptychography. The end-station is equipped with an active focusing system based on Kirkpatrick-Baez (K-B) mirror that were set in flat-mirrors configuration. Indeed, the focusing of the EUV radiation and the generation of OAM beams were performed by means of nanofabricated SZPs directly placed inside the main vacuum vessel of the end-station. The FEL light was linearly polarized in the horizontal plane with a wavelength  $\lambda$  of 18.9 nm (65.6 eV).

A sketch of the experimental setup is shown in Fig. 4.

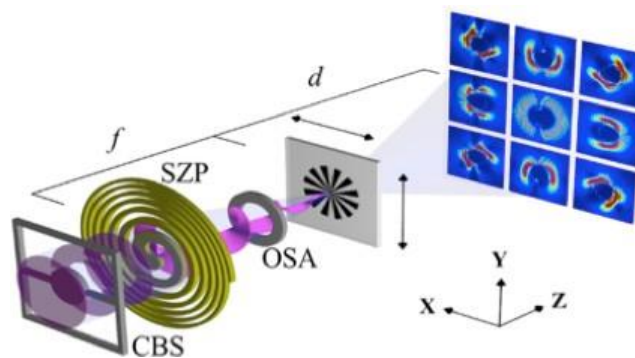


Fig. 4: Schematics of the experimental setup at the DiProI beamline. The OAM beam is generated and focused on the sample plane thanks to a spiral SZP. The order sorting aperture (OSA) allows only light from the first diffraction order to reach the sample, while the higher orders are blocked. Upstream to the SZP optics, a central beam stop (CBS) blocks the transmitted direct beam. The

sample is then scanned in the  $xy$ -plane in order to record a collection of diffraction patterns with a CCD camera, to be used for the ptychography reconstruction of both the object and the illumination functions.

Thanks to a motorized piezo stage, we were able to precisely switch between seven SZPs for the generation of  $\ell=0, \pm 1, \pm 2, \pm 3$  OAM beams. All the SZPs were fabricated with similar parameters, in order to provide a focal length  $f$  of 164.7 mm for  $\lambda= 18.9$  nm radiation, with an estimated first order focusing efficiency of about 12. An order sorting aperture (OSA) and a central beam stop (CBS) were used for spatially filtering the higher diffraction orders of the SZPs and for blocking the unfocused direct beam, respectively. Ptychography scans were performed on a 100 nm-thick HSQ Siemens star structure patterned on top of a 200 nm-thick silicon membrane.

As recently demonstrated, ptychography can be applied to characterize wavefronts on single-shot fashion at FEL sources, and it is nowadays considered a powerful metrological tool for beamline optics alignment and characterization. This important feature of ptychography reconstructions nicely combines with the high sensitivity of OAM beams to aberrations, providing a very detailed way of controlling the optimization of beamline optics. Figure 5(a) shows the ptychographic reconstructed amplitude (left-hand side plot) and phase (right-hand side plot) of the main illumination mode for  $P = -1$  when the K-B mirrors settings were not optimized.

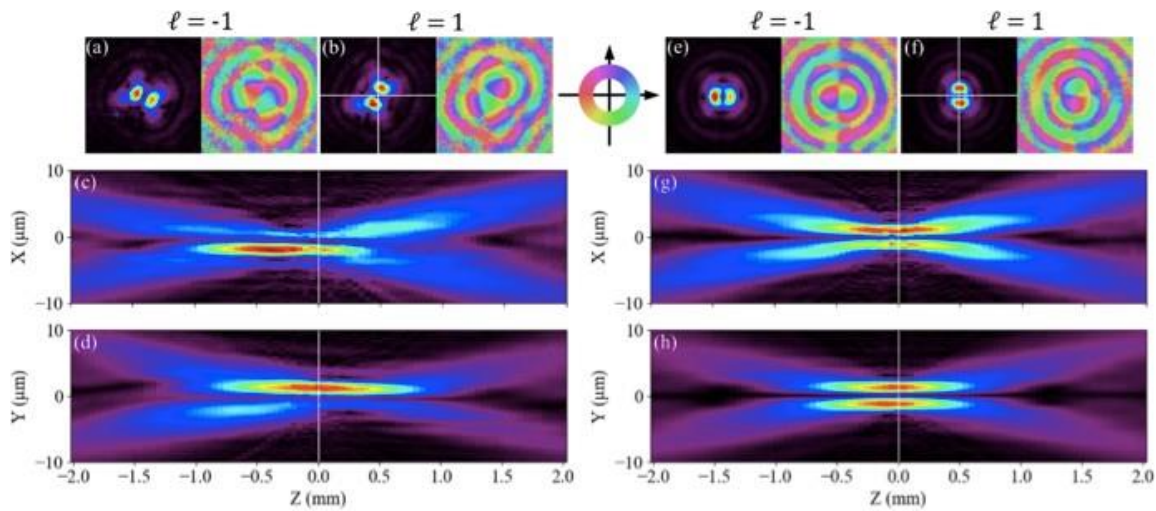


Fig. 5: Reconstructed amplitude (left) and phase (right) of the main mode for the  $\ell=-1$  illumination function when the K-B mirrors settings were not optimized. This plane defines the  $z=0$  coordinate for the following plots. (b) Similar reconstruction for the non-optimized  $\ell=1$  illumination function. (c) Section of the free-space propagation of the  $\ell=1$  reconstruction on a plane passing through the horizontal line in panel (b), corresponding to the  $xz$ -plane (top view). (d) Section of the free-space propagation of the  $\ell=1$  reconstruction on a plane passing through the vertical line in panel (b), corresponding to the  $yz$ -plane (side view). By comparing panels (c) and (d), it is possible to see a difference in the focal positions for these two projections. (e)-(h) Repetitions of plots (a)-(d) after the K-B mirrors settings where optimized for minimizing "0-degree" astigmatism. As a confirmation, panels (g) and (h) now show the same position of maximum intensity.

These plots can be compared with Fig. 5(b), which shows the reconstruction performed on the  $P = 1$  illumination. In both cases, the phase wraps continuously around  $2\pi$ , as expected for a  $P=1$  beam and the phase winding direction is opposite, as determined by the sign of  $P$ . However, the



reconstructed amplitudes show an asymmetric distribution concentrated in two lobes that rotates by approx. 90 deg while changing the phase winding direction, rather than spreading out in a “donut-like” shape as for a LG beam. We ascribe the deformation of the amplitude distribution to the residual astigmatism. The presence of “0-degree” astigmatism is confirmed by the propagation of the reconstructed illumination function along the z-axis thanks to the free-space propagator for a monochromatic wave. The results, reported in Fig. 5(c), (d) as top and side views, respectively, unequivocally show that the focal positions for these two propagations are shifted along the z-axis direction. On the other hand, Fig. 5(e)-(h) shows the results obtained with optimized K-B mirrors settings. The reconstructions show that the phase wrapping around the beam axis is maintained, and now the position of maximum intensity is approximately the same for both the projected views in Fig. 5(g), (h). The deviations at the focal plane of the reconstructed amplitude profile with respect to an ideal LG beam suggest residual “45-degree” astigmatism affecting the SZPs input illumination beam. Further experiments will be carried out in the future in order to compensate such an effect and improve OAM’s intensity profile.

## Conclusions

OAM beams with different topological charge have been generated, characterized and optimized at the FERMI FEL, using two different techniques. The latter can be easily transferred to HHG sources.

